The Endoplasmic Reticulum and Vimentin are two inter-dependent and interconnected networks

Ivo van de Pasch, 6528279

ABSTRACT
The endoplasmic reticulum (ER) is the largest organelle of a cell, and it performs multiple different functions. The diverse functions of the ER rely on its morphologically different structures. Microtubules are known to play a major role in the shaping of the ER, but the involvement of a different cytoskeletal component, the Vimentin (VIM) intermediate filament (IF) network, in this process is less well characterized. Here we found that VIM is needed to support the structure of the tubular ER network. Redistribution of VIM to the cell centre resulted in an increase in the size and number of ER sheets and a more tightly packed tubular ER network. On the other hand, re-localisation of ER membrane proteins to the periphery of the cell resulted in VIM being pulled along. Membrane contact sites of other organelles with the ER were also found to be important for the formation, maintenance, and spatial distribution of the ER morphology. The three-way junctions in the ER network also showed to play a major role in this process. Oppositely, the ER also acts as a key player in the distribution of VIM throughout the cell. These results show a direct dependency of VIM and the ER, but we also investigated the presence of indirect dependencies. We found that VIM depletion causes lysosomes to spread more throughout the cell, which could in turn affect the ER as lysosomes can reshape this organelle. Additionally, the ER is also known to affect the microtubule (MT) network, which could indirectly affect VIM, because these IFs are transported along MTs by kinesin 1. Altogether, these findings led to the conclusion that the ER and VIM networks are two interdependent and interconnected structures.

LAYMAN SUMMARY
Cells have compartmentalised their different functions in distinct organelles, which enables the cell to function as an efficient unit. The largest cellular organelle is the endoplasmic reticulum (ER); it is continuous with the nuclear envelope and contains different shapes. Closest to the nucleus, the main structure of the ER is sheets, whereas the ER appears as a tubular network in the peripheral region. These different morphologies are supported by specialised ER membrane proteins that promote these membrane structures, but the cytoskeleton also plays a key role in the shaping of this organelle. Microtubules are known to be important for this process, but we found that the intermediate filament protein Vimentin also plays a role in maintaining ER shape. When we removed Vimentin from the cell periphery by pulling it to the cell centre, the ER in these cells had a more densely packed tubular network and it also contained more and larger sheet-like structures. Additionally, we found that the Vimentin network can also be altered by the ER, so the other way around. When we pulled ER membrane proteins to the periphery, we saw that in multiple cases Vimentin was pulled along. This effect was stronger when we pulled an ER protein that stabilises the three-way junctions in the tubular network, as we saw more cells that had Vimentin pulled along with this protein. Another method we used to change the ER, was by depleting proteins that shape this organelle. When proteins that make connections of the ER with other organelles were depleted, the ER lost most of its tubular network and consisted almost entirely of sheets. The Vimentin network in these cells was retracted from the periphery, thus showing an interdependency between the two networks. The connection between Vimentin and the ER became even more apparent when we depleted cells of Atlastins, which are the proteins that mediate the fusion of ER tubules to form the three-way junctions that create the tubular ER network. This caused the ER to mainly consist of long unbranched tubules. Interestingly, we observed that these ER tubules overlapped with both microtubules and the Vimentin network, therefore really showing an interdependency between these networks. Additionally, we also aimed to investigate the possibility of an indirect effect of Vimentin on the ER. We did this because it was

described that Vimentin clusters lysosomes to the cell centre. This could then connect back to the ER because lysosomes are known to regulate the shape and distribution of the ER. We confirmed that Vimentin restrains lysosomes close to the nucleus by comparing the lysosome distribution in cells depleted for Vimentin with cells with a normal Vimentin network. In conclusion, we found that the interactions between the ER and Vimentin and contacts of the ER with other membranes are both important for the formation, maintenance, and distribution of the ER morphology. We have shown that the ER and Vimentin are two interconnected networks, which rely on each other for the maintenance of their shape and distribution in the cell.

INTRODUCTION

All eukaryotic cells have different organelles in which different processes are locally organised and executed. An organelle that performs many different functions is the endoplasmic reticulum (ER). It plays a major role in the synthesis, quality control, modification and trafficking of secretory and membrane proteins (Schwarz & Blower, 2016). In addition, the ER also plays a role in Ca^{2+} storage and release, lipid synthesis, metabolism of carbohydrates, signalling and detoxification. These different processes require distinct environments for their optimal functioning. Therefore, the ER is divided into sub-compartments; it is an extension of the nuclear envelope, in the perinuclear area the ER is mainly observed as cisternae or sheets, whereas the peripheral ER appears as a tubular network (Goyal & Blackstone, 2013; Zhang & Hu, 2016). The biosynthesis of secreted and membrane proteins is performed by ribosomes that dock onto the cisternal ER membrane, which therefore appears as rough ER (Schwarz & Blower, 2016). The other processes that are executed by the ER, like lipid synthesis and detoxification, are mainly performed in the tubular ER network, which is usually free of ribosomes.

These morphological differences of the ER are regulated by a number of shaping proteins. Some proteins promote the flat sheet-like structures of the cisternae, whereas other proteins enable the formation of the highly curved membranes of the ER tubules (Goyal & Blackstone, 2013; N. Wang et al., 2021; Zhang & Hu, 2016). To create the network of tubular ER, specialised proteins act to connect two tubules to create a three-way junction (3WJ). These 3WJs are made by Atlastin proteins (ATL), which tether the tip of a growing ER tubule to the shaft of another tubule and induce fusion of their membranes after GTP hydrolysis (S. Wang et al., 2016; Zhou et al., 2019). Next, Lunapark proteins (Lnp) are attracted to this newly formed 3WJ, which stabilises the junction.

Besides the proteins that shape the membranes of the ER, the morphology of this organelle is also highly dependent on the cytoskeleton. A lot is already known about the importance of microtubules (MTs) in the shaping of the ER (Goyal & Blackstone, 2013). In the absence of MTs, most ER tubules collapse and turn into sheets (Guo et al., 2018). MTs play a major role in the dynamics of the ER network (Waterman-Storer & Salmon, 1998); the ER tubules can grow by attaching to the MT plus end with the Tip Attachment Complex (TAC) and follow the growing and shrinking MTs. Another mechanism, called sliding, involves motor proteins that drag ER tubules along MTs. There is also a mechanism in which the ER is remodelled by hitchhiking on different organelles, like mitochondria and lysosomes, that are being transported along MTs (Guo et al., 2018; Lu et al., 2022). The ER is attached to these and other organelles through membrane contact sites (MCS). Proteins of the VAP (vesicle-associated membrane protein (VAMP) associated protein) family play a major role in establishing these contacts, as they connect the ER to the plasma membrane, mitochondria, Golgi, late endosomes, lysosomes and peroxisomes (Helle et al., 2013; James & Kehlenbach, 2021; Wu et al., 2018). Importantly, there is also a MT dependency on the ER, since ER dynamics affect the distribution and bundling of MTs (Tikhomirova et al., 2022).

However, MTs are not the only cytoskeletal component that affects the ER. The intermediate filament protein Vimentin (VIM) has been shown to be essential for the spreading of the endoplasm (Lynch et al., 2012). VIM is a type III intermediate filament protein that is widely studied for its role in cell migration and metastasis in cancer. VIM plays an important role in protecting the nucleus from rupturing during cell migration (Patteson et al., 2019). The VIM network is flexible when there is few strain, but when high strain is applied the network hardens (Janmey et al., 1991), suggesting that VIM plays an important role in maintaining cellular integrity when a cell is under high mechanical stress.

The distribution of VIM is dependent on MTs as it is transported by kinesin 1 (Robert et al., 2019). Additionally, RNF26, an ER membrane protein, has been described to link VIM to the perinuclear ER, suggesting a role for VIM in the maintenance of the ER morphology (Cremer et al., 2022). Another possible linker of VIM and the ER could be Nuclear envelope spectrin-repeat protein-3 (Nesprin-3) in combination with Plectin, since it has been shown that these proteins link VIM to the nuclear envelope (Ketema et al., 2013). This, in combination with results showing that Nesprin-3 is occasionally found in the perinuclear ER, hints to a possible linkage between the ER and VIM. Besides these examples, it is likely that more linkers exist and are yet to be described.

Despite that the ER and VIM are both widely studied separately, their interdependencies are not well known. Until now, only one linker has been described to link VIM to the ER membrane (Cremer et al., 2022). We were interested in how changes in the VIM network affect the morphology of the ER and the other way around. We found that a loss of VIM in the cell periphery, by pulling it to the cell centre with a rapalog-inducible heterodimerisation system, resulted in an increase in the number of sheets observed in the peripheral area of the cell. We also observed that disruption of the ER by either relocalisation or knock-down of ER shaping proteins affects the VIM and MT networks. Pulling of the ER proteins Sec61β and Lnp resulted in the presence ER sheets in the cell periphery and VIM being pulled along with these proteins. Knock-down of MCS establishing proteins VAP A and VAP B caused an almost complete loss of ER tubules and a more centrally clustered appearance of VIM. Depletion of ATLs, the proteins that mediate fusion of ER tubules to create 3WJs, resulted in an ER network mainly consisting of long unbranched tubules, which showed great overlap with both MTs and VIM. Therefore, we have shown that the ER and VIM are two interdependent networks.

RESULTS

Vimentin and ER networks overlap

To characterize the spatial distribution of VIM and the ER network, we performed immunofluorescence (IF) staining and observed the subcellular location of VIM and the ER. COS7 cells were fixed and co-stained for Vimentin and Calnexin, a total ER marker. To examine whether VIM and the ER co-align, we analysed the normalised intensity of the individual channels in the cell periphery. Comparing both VIM and ER networks it is notable that these networks are most dense in the perinuclear region, whereas these networks are sparser in the periphery (Fig. 1A). It is also observable that both networks overlap to some extent, which is confirmed by the line intensity plot (Fig. 1B). Despite that both VIM and the ER are more sparse in the periphery, they do not only overlap in the perinuclear area (Cremer et al., 2022), but also in the periphery, which hints towards the possibility that these networks are connected.

Depleting peripheral Vimentin causes an increase in number and size of ER sheets

To further investigate the role of peripheral VIM, we used the rapalog-inducible heterodimerisation system to relocalise VIM to the cell centre, thus depleting it from the periphery. We transfected COS7 and HeLa cells with constructs encoding 2xFKBP-mCherry-VIM and FRB-TagBFP-GCN4-ppKin14Ulb,

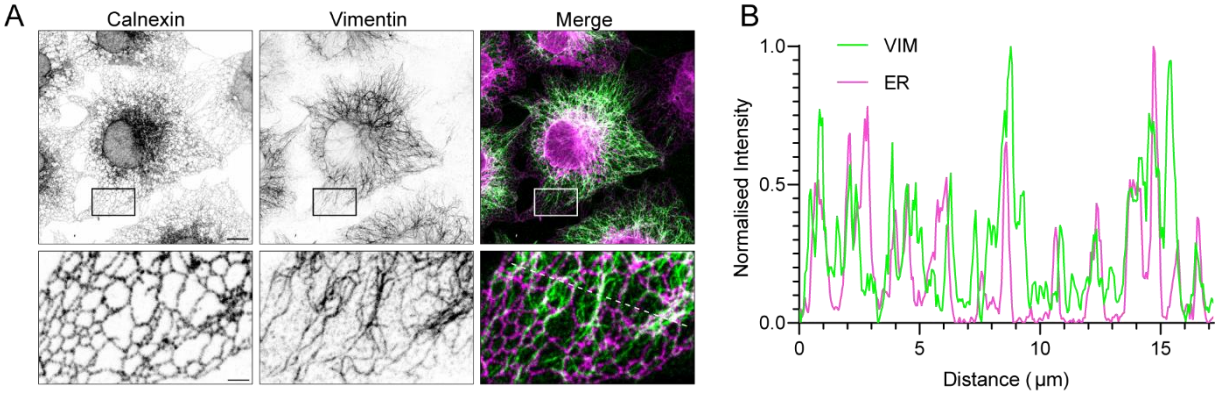

Figure 1 Vimentin colocalises with the Endoplasmic Reticulum. (A) Immunofluorescence images of COS7 cells stained for Calnexin (magenta) and Vimentin (green). Boxes indicate the areas shown in the zoom-ins. Scale bar 10 µm, zoom-in 2 µm. (B) Line intensity plot along the dotted white line in (A). All intensity values were subtracted by the background signal and normalised to the highest value for the corresponding channel.

which dimerise upon the addition of rapalog, resulting in microtubule minus-end directed transport of VIM by plant Kinesin-14 (pK14). Without rapalog added, VIM was able to extend to the cell periphery and the peripheral ER appeared as a tubular network with relativily large polygons and a few small sheets (Fig. 2A). However, when the cells were treated with Rapalog for 2 hours and VIM was therefore clustered perinuclearly, the ER morphology changed; the tubules were more densely packed and there were more sheet-like structures present in the peripheral region. Besides the differences in the ER morphology, the MT network was also affected by the repositioning of VIM, as the MTs looked dis-organised. Because MTs are known to play a major role in the shaping of the ER, we cannot address if the effect of VIM repositioning on the ER is a direct effect or an indirect effect through MTs.

Therefore, we aimed to remove MTs and assess the role of VIM alone on the ER network, by depolymerising them with nocodazole. However, when all MTs are depolymerised, the ER network collapses into a structure that is almost exclusively consisting of very large sheets. So, to maintain the regular ER morphology, but reduce the effect MTs can have on the ER, the cells were treated with nocodazole for either 2 or 4 minutes, an amount of time in which no significant changes in MT density could be measured (Fig. 2B). In cells with a normal VIM distribution that were treated with nocodazole, it could be observed that the ER still posessed a tubular network with large polygons and few peripheral sheets (Fig. 2A). It should be noted that the perinuclear ER cisternae seemed to cover a larger part of the cell than in cells not treated with nocodazole and thus these cells also had a slighty smaller tubular ER network. When we treated cells that have VIM repositioned to the centre with nocodazole, we observed a similar and sligthly more severe phenotype than in the cells not treated with nocodazole, larger and more ER sheets and smaller polygons. This points towards a direct effect of VIM on the ER morphology. We also examined the effect of these treatments on the cell size and shape and we found that the pulling of VIM to the perinuclear area, and to a lesser extent the short microtubule depolymerisation, resulted in smaller and more rounded cells (Fig. 2C & D). This indicates that VIM plays an important role in cell spreading. We found that these results were not cell-specific; the effects seemed to be more pronounced in COS7 cells (Fig. 2), but we observed similar results in HeLa cells (Fig. S1). To summarise, VIM is not important for the spreading of the ER network, but it plays a key role in the maintenance of the ER morphology, specifically the polygonal network.

Vimentin clusters lysosomes perinuclearly

Recently, it was described that VIM plays a role in the clustering of lysosomes to the cell centre (Cremer et al., 2022). This finding could be relevant for this study because lysosomes can remodel and reshape the ER (Lu et al., 2022). To understand if VIM could affect the ER indirectly through lysosomes, we first wanted to confirm the findings about the interplay between VIM and lysosomes. We did this by depleting cells for VIM and comparing their lysosome distribution with the control condition. The radial lysosome distribution was quantified by determining the relative distance of every lysosome to the cell centre. In HeLa cells, lysosomes are located relatively close to the nucleus (Fig. 3A & B). However, when VIM was depleted the lysosomes appeared more spread thoughout the cell, implying a role for VIM in restricting the lysosomes to a perinuclear organisation.

To confirm this, we also determined the lysosome distribution in MCF7 cells, which normally do not express VIM (Fig. 3C). The lysosomes in these cells are spread throughout the whole cell and no perinuclear clusters of lysosomes could be observed (Fig. 3C & D). When mNeonGreen-VIM was expressed in these cells, we found that the lysosomes in these cells were not spreading around the whole cell anymore, but they were confined to the perinuclear region. These results led to the conclusion that VIM clusters lysosomes to the perinuclear area and prevents their speading to the periphery. This function of VIM could have an indirect effect on the ER, as lysosomes have been shown to remodel the ER morphology (Lu et al., 2022), but this will need further investigation.

Pulling of ER proteins to the periphery affects the VIM network

After having shown that the ER is dependent on VIM to maintain its morphology, we aimed to investigate the dependency of VIM on the ER. We did this by using the rapalog-inducible hetero-dimerisation system to pull Sec61β either to the cell centre with pK14 or the periphery with KIF5A.

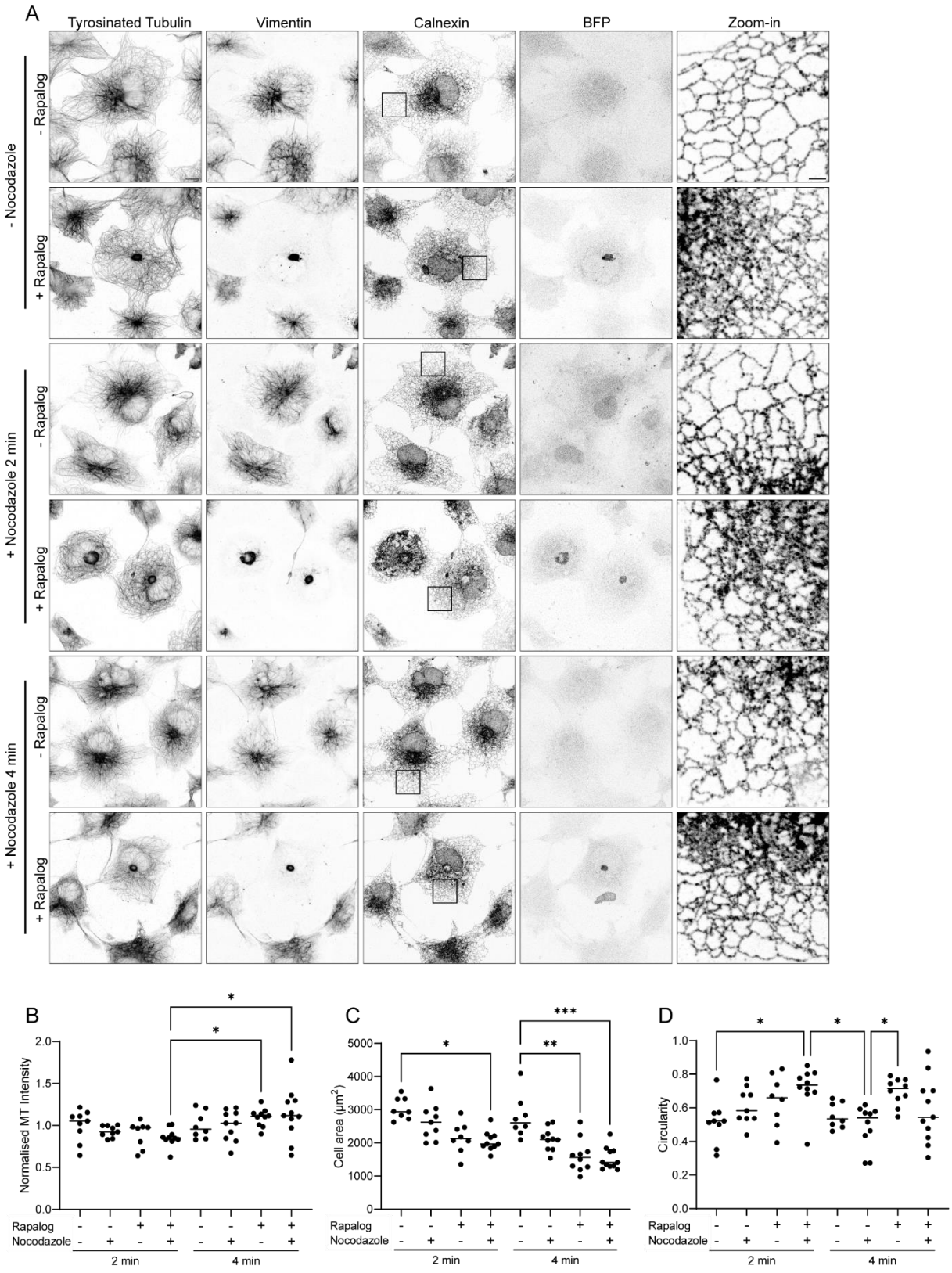

Figure 2 The number and size of ER sheets increases when Vimentin is repositioned to the cell centre and microtubules are depolymerised shortly. (A) Immunofluorescence images of COS7 cells transfected with 2xFKBP-mCherry-Vimentin and FRB-TagBFP-GCN4-ppKin14Ulb and stained for tyrosinated tubulin, Vimentin and Calnexin. The cells were treated with Rapalog (1.5 hours) and Nocodazole (2 and 4 minutes) on ice, indicated on the side. The boxes indicate the areas shown in the zoom-ins. Scale bar 10 µm, scale bar zoom-in 2 µm. (B) Quantification of the microtubule intensities, normalised to the cells treated with neither of the compounds. (C) Quantification of the cell area. (D) Quantification of the cell circularity. In the graphs, only significant differences are indicated. * P<0.05, ** P<0.01, *** P<0.001.

Sec61β is a trans-membrane protein that is part of the translocon complex, and it is present throughout

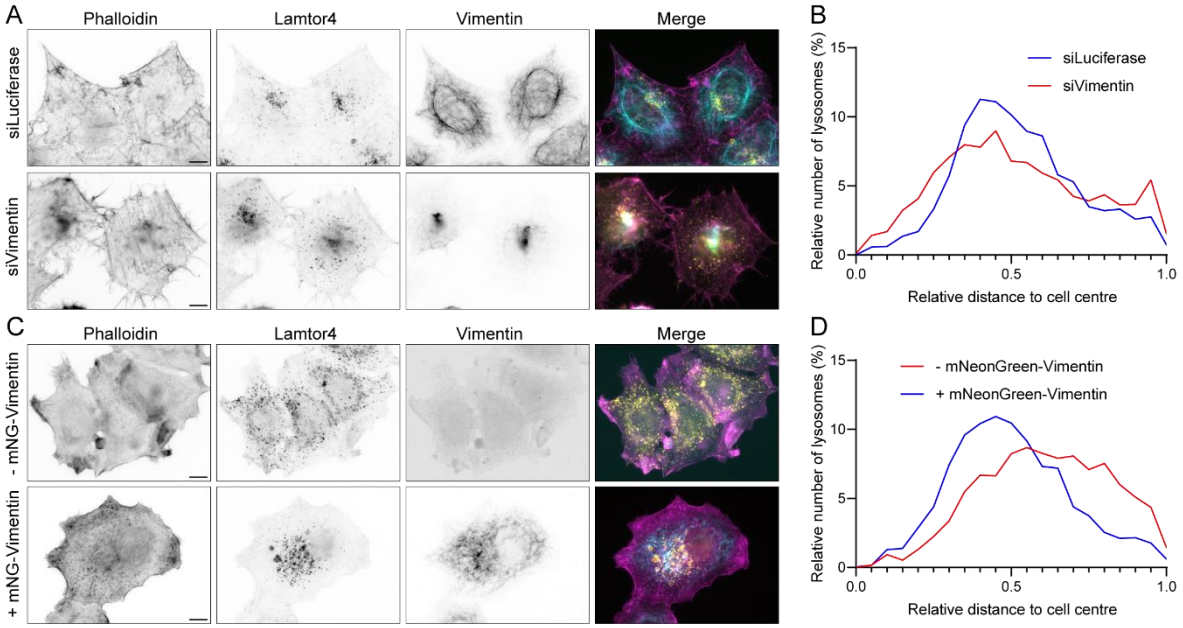

Figure 3 Vimentin clusters lysosomes to the perinuclear region. (A) Immunofluorescence images of HeLa cells treated with the indicated siRNA and stained for phalloidin (magenta), lamtor4 (yellow) and vimentin (cyan). Scale bar 10 µm. (B) Quantification of the lysosome distribution in cells of the KD experiment in (A). On the x-axis, 0.0 indicates the cell centre and 1.0 resembles the plasma membrane. (C) Immunofluorescence images of MCF7 cells transfected with or without mNeonGreen-Vimentin and stained for phalloidin (magenta), lamtor4 (yellow) and vimentin (cyan). Scale bar 10 µm. (D) Quantification of the lysosome distribution in cells of the VIM rescue experiment in (C). On the x-axis, 0.0 indicates the cell centre and 1.0 resembles the plasma membrane.

the whole ER. When Sec61β was relocalised perinuclearly in pK14 transfected cells by treating these cells with Rapalog for 2 hours, we did not observe major changes in the ER morphology, as seen in the IF images of the total ER marker Calnexin (Fig. 4A). Additionally, both MT and VIM networks were not affected by this pulling of Sec61β to the cell centre (Fig. 4A & B). By comparing the normalised intensity values of the cytoskeletal networks in the cells, no significant changes in MT or VIM density were observed (Fig. 4C & D). Neither did we observe changes in the distribution of VIM (Fig 4E), which was quantified by dividing the area of VIM spreading by the total cell area. In contrast to this, redistribution of Sec61β to the periphery dramatically affected the ER morphology; the ER cisternae that normally reside perinuclearly were now located at the cell edges (Fig. 4A). The MT network appeared disorganised in these cells, but this was also the case in the cells that were not treated with rapalog and thus had a regular ER morphology. Since there was also no difference in MT intensity between the cells treated with or without rapalog (Fig. 4D), we think that the MT disorganisation could be caused by over-expression of the rapalog-inducible KIF5A motor that was used this experiment, although we cannot be certain that the cells are actually transfected with the motor protein. However, it could also be caused by over-expression of Sec61β, because we also observed disorganised MT networks in the cells expressing Sec61β and pK14. The VIM network also seemed to be affected, but this differed from cell to cell (Fig. 4B). In some cells VIM was pulled along with Sec61β in every direction, in most of the cells VIM was only pulled along in a few directions, but there were also cells in which VIM was not pulled along with Sec61β at all (Fig. 4F & S3). This shows that there is a dependency of VIM on the ER, but it does not seem to be dependent directly on Sec61β. When looking at cell size and shape, we did not observe significant changes caused by the pulling of this general ER membrane protein in COS7 cells (Fig. 4G & H). However, in HeLa cells it appeared as if the cells that have Sec61β pulled to the centre were smaller and more rounded, whereas cells with Sec61β pulled to the periphery were less spherical (Fig. S2G & H). This seemed to be the only difference between these cell types, since all other results were similar (Fig. S2). Thus, we found that VIM is sometimes pulled along with Sec61β, a general ER membrane protein, when in it pulled to the cell periphery, implying a direct connection between the ER and VIM.

Now we know that changes in the ER morphology affect the VIM network, we explored to find a more direct cause of this dependency. We hypothesised that Lnp would be a promising candidate, because it has been shown to stabilise the 3WJs in the tubular ER network (Chen et al., 2015). We

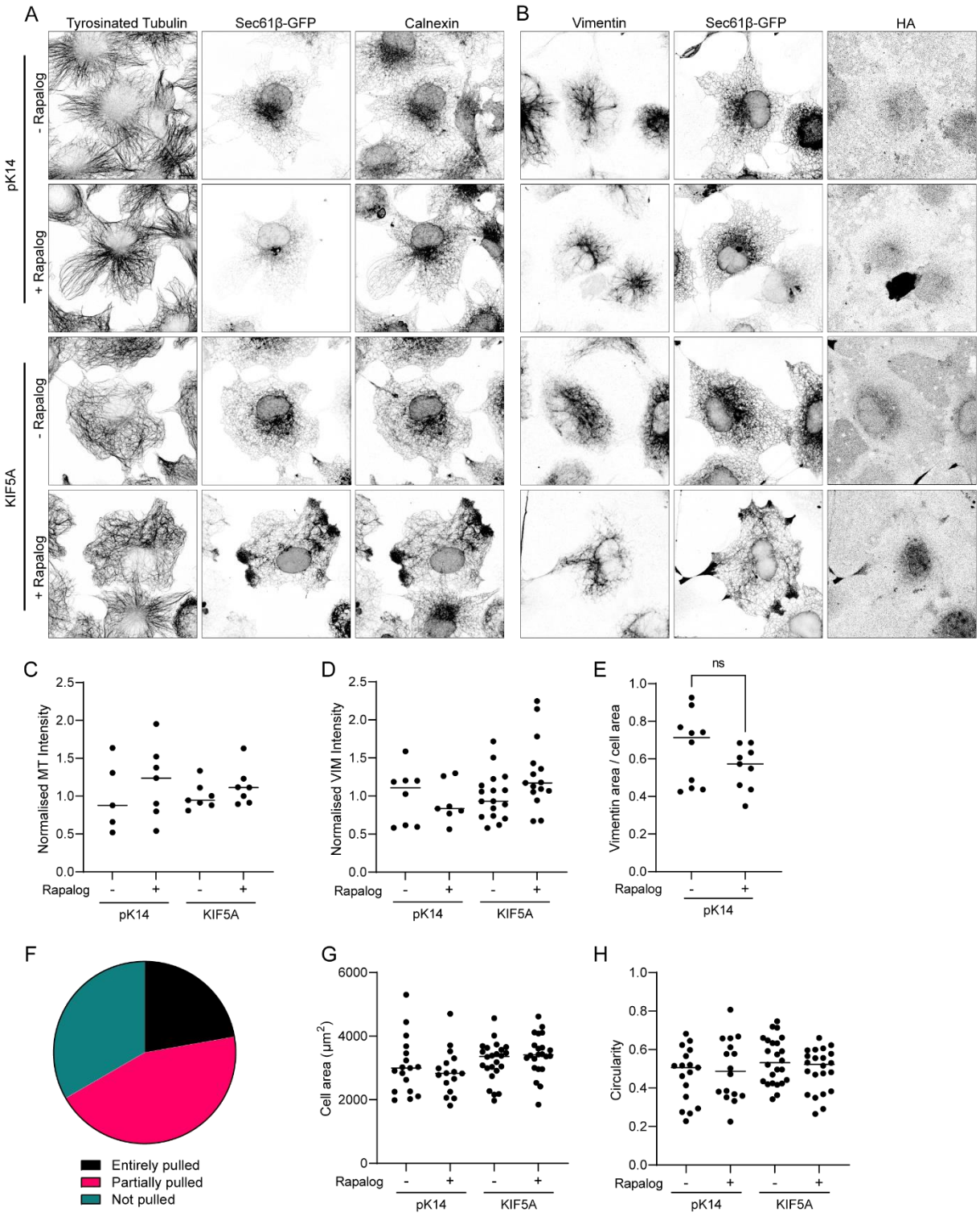

Figure 2 Repositioning the general ER membrane protein Sec61β to the cell periphery affects the Vimentin network. (A) Immunofluorescence images of COS7 cells transfected with GFP-FKBP-Sec61β and either FRB-HA-GCN4-ppKin14 or HA-KIF5A-FRB and stained for tyrosinated tubulin, GFP and Calnexin. The cells were treated with Rapalog for 2 hours to induce translocation. Scale bar 10 μm. (B) Same as in (A), but here stained for Vimentin, GFP and HA. (C) Quantification of the microtubule intensities normalised to the cells not treated with Rapalog. (D) Quantification of the Vimentin intensities normalised to the cells not treated with Rapalog. (E) Quantification of the Vimentin spreading in the cells transfected with the rapalog inducible pK14 motor. (F) Distribution of the different observed phenotypes regarding the Vimentin network being pulled along with Sec61β (n=18). (G) Quantification of the cell area. (H) Quantification of the cell circularity.

hypothesise that VIM could play a role in this process by binding to Lnp and keeping it in position, preventing its movement. So, to investigate the possible interaction of these two proteins, we repeated the previous experiment, but here we repositioned Lnp instead of Sec61β. Again, no major differences could be observed in the ER morphology as well as the MT organisation and density when

Lnp was relocated perinuclearly (Fig. 5A & C). The VIM network was slightly affected, as we observed some cells that showed a stronger connection between VIM and Lnp, since in those cells VIM was located more centrally in the cell, co-pulled with Lnp. We think there might be a tendency of VIM being pulled along to the centre with Lnp, although no significant changes in VIM density and distribution

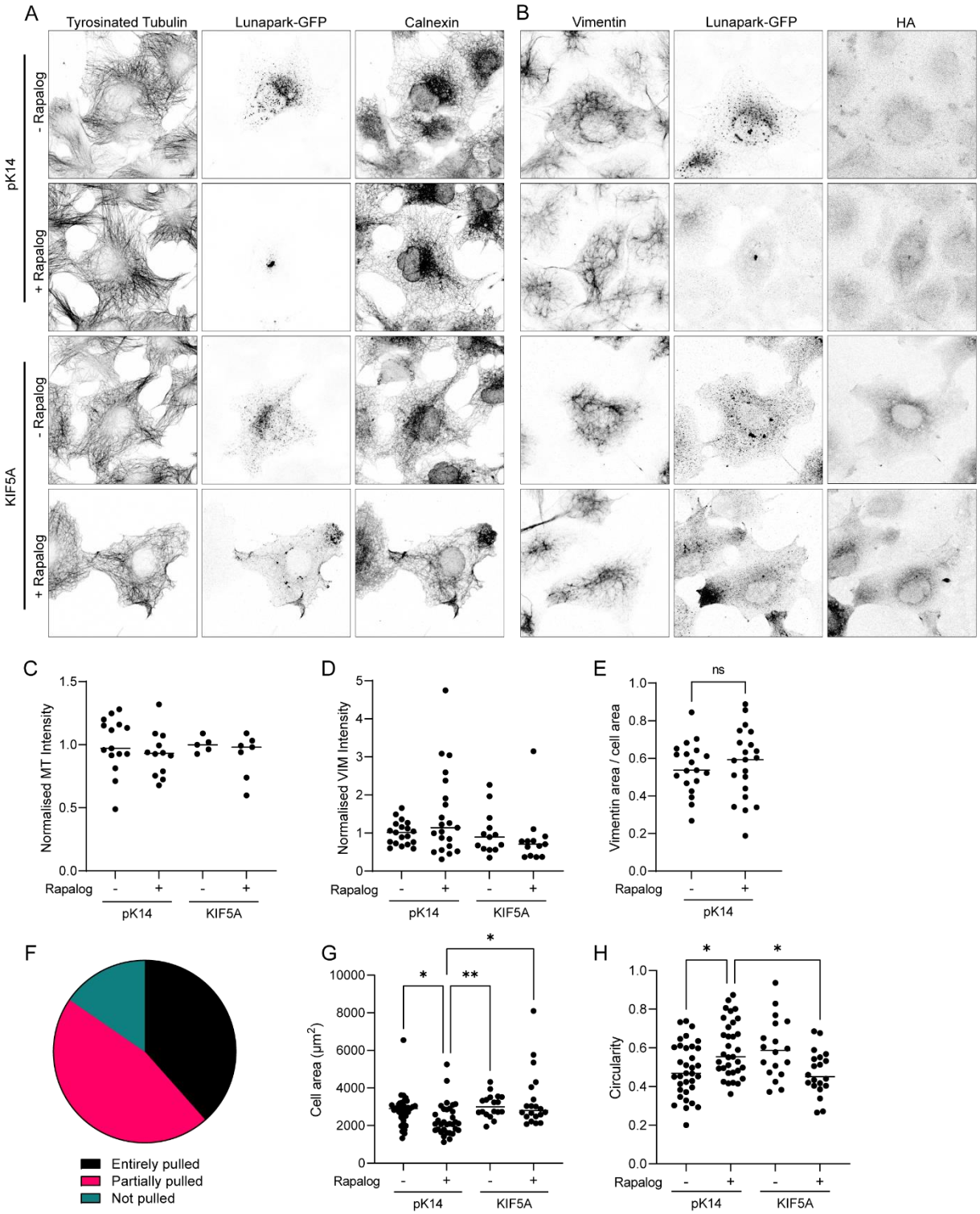

Figure 3 Repositioning Lunapark to the cell periphery affects the Vimentin network. (A) Immunofluorescence images of COS7 cells transfected with LNP-GFP-2xFKBP and either FRB-HA-GCN4-ppKin14 or HA-KIF5A-FRB and stained for tyrosinated tubulin, GFP and Calnexin. The cells were treated with Rapalog for 2 hours to induce translocation. Scale bar 10 µm. (B) Same as in (A), but here stained for Vimentin, GFP and HA. (C) Quantification of the microtubule intensities normalised to the cells not treated with Rapalog. (D) Quantification of the Vimentin intensities normalised to the cells not treated with Rapalog. (E) Quantification of the Vimentin spreading in the cells transfected with the rapalog inducible pK14 motor. (F) Distribution of the different observed phenotypes regarding the Vimentin network being pulled along with Lunapark (n=13). (G) Quantification of the cell area. (H) Quantification of the cell circularity.

could be measured (Fig. 5B, D & E). However, when Lnp was pulled to the periphery, the ER network was affected in a similar manner as with the pulling of Sec61β; loss of the perinuclear cisternae and sheet-like structures at the positions were Lnp is accumulated (Fig. 5A). We also observed that the MT network was disorganised again, most likely caused by KIF5A or Lnp overexpression, as we did not see differences between cells treated with or without rapalog (Fig. 5A & C). Similar to the previous experiment, we again observed three different phenotypes when comparing the different degrees of VIM being pulled along with Lnp (Fig. 5B & S3). However, the distribution was different; there were more cells that had VIM pulled along with Lnp in all directions and less cells with VIM not pulled along at all, compared to the results of the pulling of Sec61β (Fig. 4F & 5F). This indicates that Lnp could be linking VIM to the ER, as affecting the location of this protein had a stronger effect on VIM than relocalising a general ER protein. Also when looking at cell size and shape, we measured more significant changes in COS7 cells with Lnp redistributed than Sec61β. Pulling of Lnp to the periphery resulted in less circular cells, whereas relocalisation to the cell centre resulted in smaller and more rounded cells, something we also observed in cells with VIM relocated perinuclearly, thus strengthening the correlation of their interaction. Altogether, we have shown that relocalisation of Lnp has a stronger effect on the VIM distribution than the pulling of Sec61β, thus hinting to a more direct connection between VIM and the 3WJs of the ER network.

Depletion of ER shaping proteins affects the Vimentin network

Since we found that changing the ER morphology by redistributing ER membrane proteins affects the VIM network, we were interested to examine if changing the ER morphology with a different method also affects the VIM network. We did this by depleting different ER shaping proteins using siRNAs. When we depleted proteins of the VAP family (VAP A and VAP B), which the ER needs to establish MCSs with many different organelles, including the plasma membrane, the ER lost most of its tubular network and most of the ER appeared as sheets (Fig. 6A). This did not affect the density of the MT and VIM networks (Fig. 6B & C), but the distribution of VIM was different; VIM was less spread throughout the cell and remained located more perinuclearly (Fig. 6D). The depletion of these VAP proteins did not affect the cell size and shape (Fig. 6E & F). Most of these results in COS7 cells could be replicated in HeLa cells, except the change in the spreading of VIM, which did not change in HeLa cells (Fig. S4). To summarise, loss of membrane contact sites of the ER with other organelles, by VAP depletion, resulted in a loss of tubular ER and a retraction of VIM from the cell periphery.

Because we identified Lnp to play a role in the dependency of VIM on the ER, we wanted to further investigate the role of 3WJs in connecting VIM to the ER. Therefore we depleted cells for different ATL proteins, which mediate the fusion of ER tubules to make a three-way junction. In cells depleted for ATL2, the ER lost most of its perinuclear cisternae and mainly consisted of long unbranched tubules (Fig. 6A). These ER tubules mainly seemed to follow the structure of the MT network. Interestingly, the VIM network also showed overlap with these two networks. The structural similarities were the most interesting results in these cells depleted for ATL2, as no significant differences were observed in the densities of the MT and VIM networks, as well as the cell size and shape (Fig. 6B, C, E & F). Cells depleted for ATL3 showed a less severely affected ER compared to the cells depleted for ATL2, but nevertheless the overlap of the ER with the MTs was still apparent (Fig. 6A). It could be that the level of depletion was lower in the cells depleted for ATL3, but it has been shown before that ATL3 KD has a weaker effect on the ER morpology than ATL2 KD, and that ATL2 is better able to rescue the observed phenotype compared to ATL3 (Hu et al., 2015). In these cells, VIM was affected differently, compared to ATL2 KD cells, as here VIM was retracted from the periphery and did not spread far throughout the cell (Fig. 6D). We also performed a double depletion of both ATL2 and ATL3, and in those cells the ER was affected most severely, with an almost complete loss of ER sheets and rarely any three-way junctions to be detected (Fig. 6A). Strikingly, the overlap between the ER, MTs and VIM was very clear in these cells, showing that all three networks are interconnected. We hypothesise that the morphological changes in the ER network, caused by the depletion of ATL2 and ATL3, result in a disorganised MT network, because it has been shown that the ER directly affects MTs

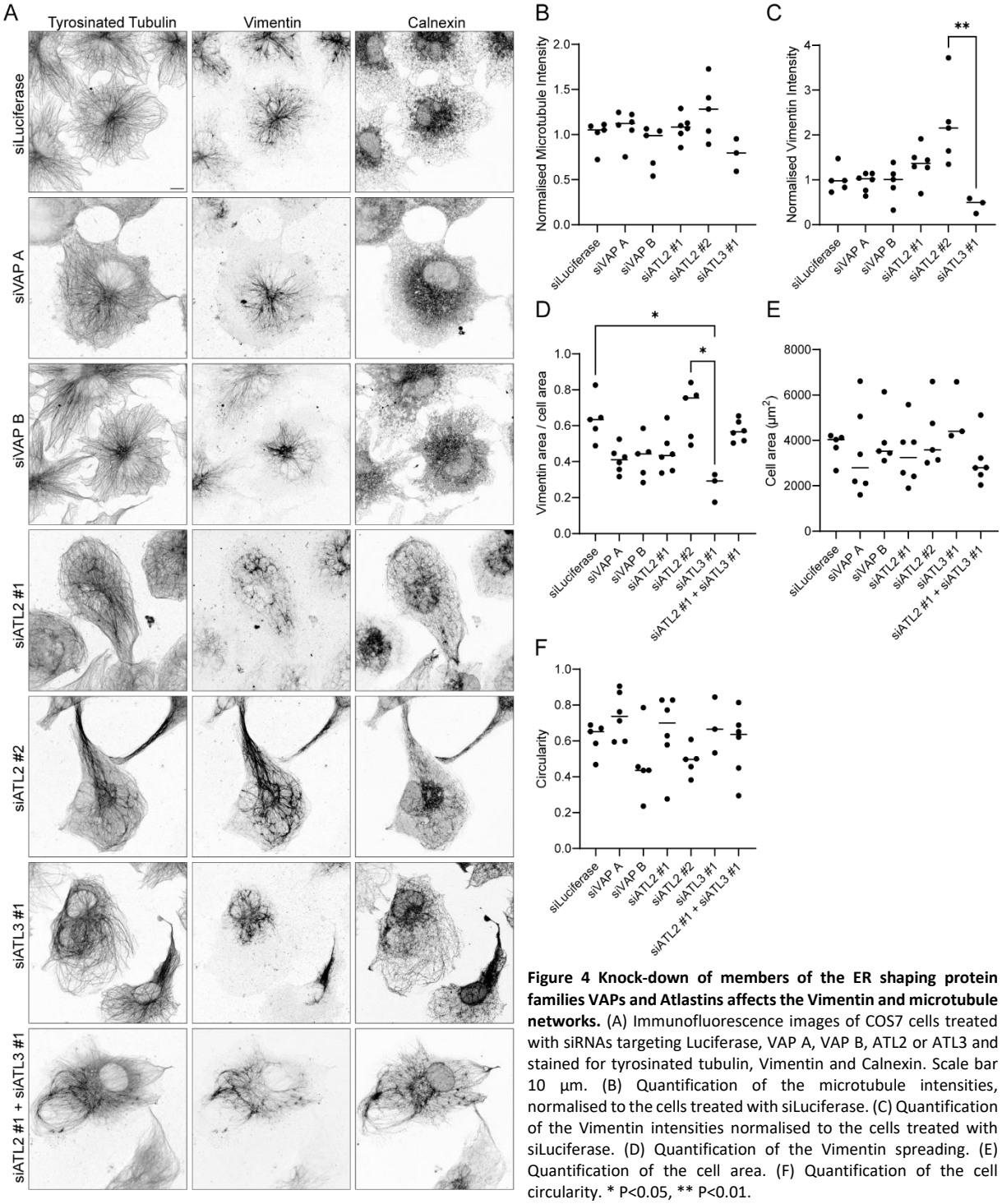

Figure 4 Knock-down of members of the ER shaping protein families VAPs and Atlastins affects the Vimentin and microtubule networks. (A) Immunofluorescence images of COS7 cells treated with siRNAs targeting Luciferase, VAP A, VAP B, ATL2 or ATL3 and stained for tyrosinated tubulin, Vimentin and Calnexin. Scale bar 10 µm. (B) Quantification of the microtubule intensities, normalised to the cells treated with siLuciferase. (C) Quantification of the Vimentin intensities normalised to the cells treated with siLuciferase. (D) Quantification of the Vimentin spreading. (E) Quantification of the cell area. (F) Quantification of the cell circularity. * P<0.05, ** P<0.01.

(Tikhomirova et al., 2022). Since VIM is transported throughout the cell by kinesin 1 (Robert et al., 2019), this could explain the overlap of all three networks. In HeLa cells the effects of ATL depletion were less severe than in COS7 cells. The ER maintained most of its perinuclear cisternae in HeLa cells and there were more 3WJs present than in COS7 cells (Fig. S4A). Both in HeLa and COS7 cells the MT network was disorganised upon ATL depletion, but the overlap with the ER was much less apparent in HeLa cells. The VIM network in HeLa cells mainly overlapped with the dense sheet-like structures of the ER in the ATL depleted cells, whereas in COS7 it also showed great overlap with the ER tubules. Altogether, we found that depletion of ER proteins resulted in changes in the VIM and ER networks. Knock-down of ATLs resulted in long, unbranched ER tubules and a more spread VIM network that co-aligned with both the ER and MTs. The ER network seems to be interconnected with MTs and VIM,

because changes in the ER affect the VIM distribution and the radiality of the MT network. It appears that the presence of ER tubules is important for the spreading of the VIM network, because in the absence of ER tubules, the cell periphery is devoid of VIM.

DISCUSSION

This work provides insights into the interdependencies of the ER and the VIM network. We found that the ER does not only show overlap with the VIM network in the perinuclear area as was described before (Cremer et al., 2022), but also in the peripheral region. Removing VIM from the periphery by relocalisation with a rapalog-inducible heterodimerisation system resulted in a more densely packed tubular ER network with smaller polygons and more sheet-like structures. We tried to rule out the effect of the MTs by shortly depolymerising them with nocodazole, which slightly enhanced the affected ER phenotype. We also found that pulling ER proteins to the periphery affects the VIM network, as in some cases VIM was pulled along with the ER protein. VIM was more sensitive to the pulling of the 3WJ stabilising protein Lnp than a general ER protein (Sec61β), hinting towards a possibly more specific connection between the ER and VIM. Depletion of the ER proteins that make the MCSs with other organelles (VAP A/VAP B) caused an almost complete loss of the tubular ER network, leaving the main ER morphology to be sheets. In these cells, the VIM network was retracted from the periphery, thus only spreading into the perinuclear region. KD of ATLs resulted in a loss of the network structure of the ER, that mainly consisted of long unbranched tubules. These ER tubules showed strong overlap with both MTs and the VIM network. Additionally, the VIM network also appeared more spread in the ATL depleted cells, compared to the control. Altogether, these results show that not only the ER and MT networks are interdependent, but also VIM is interdependent and interconnected with these networks.

The VIM IF network is most widely known for its mechanical function in regulating cell shape and maintaining cellular integrity (Patteson et al., 2019). Here we describe that VIM is also important for supporting the different morphologies of the ER. Besides this mechanical role, VIM could also have a functional role, by reducing ER dynamics locally, enabling the possibility for the ER to maintain long-lasting interactions with other organelles. We have already observed that obstructing the formation of MCSs affects the VIM distribution, it could be that VIM plays a role in the formation and maintenance of MCSs. Therefore, it would be interesting to further investigate the functional role that VIM exerts on the ER. VIM could also be important for preventing ER stress, since it provides stability.

MTs are known to play a major role in the dynamics of the ER and without them, the whole ER collapses into sheets (Guo et al., 2018; Waterman-Storer & Salmon, 1998). The distribution of VIM is also dependent on MTs, as it is distributed by kinesin 1 (Robert et al., 2019). Therefore, it is very likely that the increased size and number of ER sheets we observed when we pulled VIM to the cell centre (Fig. 2), are also partially a result of an indirect effect through MTs. We found that redistribution of VIM to the cell centre caused a disorganisation in the MT network, which could in turn affect the ER morphology. Even though we aimed to rule out the role of MTs, the short depolymerisation with nocodazole did not result in a significant loss in MT density. Therefore, we cannot ignore a possible indirect effect on the ER by MTs, as we know that the number of ER sheets increases upon MT depolymerisation. However, we did notice that the effect of MTs on the ER is greater when we pulled VIM to the cell centre. Additionally, in the cells where the different ER proteins were redistributed to the periphery, the MT network also appeared disorganised (Fig. 4 & 5). However, since this is also observed in cells treated without rapalog, the MT disorganisation is possibly caused by overexpression of the rapalog-inducible KIF5A motor. We also observed MT disorganisation in the cells transfected with pK14, although less apparent, this could also mean that the overexpression of ER proteins causes MT disorganisation, as it is known the ER can affect the distribution of MTs (Tikhomirova et al., 2022). When we compare the ER morphology of these untreated cells transfected with KIF5A with the ER of cells transfected with pK14, there were minor differences in the ER morphology, as the polygons appeared to be smaller and there were more sheet-like structures in the periphery of the KIF5A overexpressing cells. To gain a better understanding of the flow of events and to figure out if the results

we got are a result of direct or indirect effects, it would be interesting to perform these experiments with live-cell imaging.

When comparing the rapalog-induced redistribution of the ER proteins to the different locations, it is interesting that pulling to the centre did not lead to significant changes, whereas pulling to the periphery led to drastic changes in not only the ER morphology, but also the VIM distribution. We hypothesise that this happens because the rapalog-induced pulling of proteins causes accumulation of high numbers of proteins. In the native condition, the perinuclear ER is relatively dense, compared to the peripheral ER. Therefore, relocalising ER proteins to the centre more closely resembles the native state, whereas pulling to the periphery was found to result in an opposite ER morphology, with the sheets at the periphery and perinuclear ER tubules. The effect of these experiments on the VIM network can be explained by assuming that the ER morphology is a key player in determining the VIM distribution, and not necessarily the redistribution of a specific protein. Thus, since relocalising ER proteins to the cell centre did not affect the ER morphology, this explains why we did not observe a more retracted VIM network, something that would be expected when a protein that binds VIM was pulled to the cell centre. Relocalisation of ER proteins to the periphery severely affected the ER morphology, and there we also observed changes in the VIM network. However, we did not observe a phenotype where VIM is pulled along in all directions with the redistributed ER protein in all cells, what might be expected for a linker protein. We found that the presence of ER tubules is important for the spreading of VIM throughout the cell and we hypothesise that there could be a connection between VIM and the 3WJs of the ER network, because VIM was pulled along more frequently with Lnp compared to Sec61β. In addition, redistribution of LNP to the cell centre resulted in smaller and more rounded cells, which was also observed for cells with VIM pulled perinuclearly, whereas this was not the case for Sec61β, thus pointing towards a connection of 3WJs and VIM. If this linker would be Lnp, it would mean that this is a reversible anchoring of the ER 3WJ to VIM, since VIM is not pulled along with Lnp in every event. A reversible linkage could explain the observed phenotypes, because the events where VIM is not pulled along with Lnp could be a result of instances where the pulled Lnp was not bound to VIM, or it could be that the binding loosened and that VIM got retracted from the periphery and was not able to bind again to the Lnp that was accumulated in the periphery. The finding that VIM is not affected in the experiment where Lnp is relocalised to the centre, can be explained by the possibility that endogenous Lnp, which could not be detected, is still present thoughout the ER and links this organelle to the VIM network in the peripheral region. In the case of Sec61β relocalisation to the periphery, VIM could be pulled along because Lnp, or another linker, is accidentally also pulled along with Sec61β. This hypothesis of Lnp providing a reversible link between the ER and VIM could also hold in the ER protein KD experiment. In the case of VAP depletion, most 3WJs are lost, which could result in a more perinuclear organisation of Lnp. The phenotype observed in the ATL2/3 double depleted cells could be explained by the loss of 3WJs and the ability to make new ones. Therefore, Lnp is unable to localise to 3WJs and might be present throughout the ER, explaining the more spread VIM network. The tubular appearance of the ER in these cells makes it more clear that the ER and VIM are connected.

However, in ATL3 depleted cells a strongly retracted VIM network was observed. Even though this is a preliminary result based on a few cells, we think ATL3 could be another possible linker of the ER to VIM. Its absence could be the reason why the VIM network cannot spread throughout the cell. And because this protein is also localised to 3WJs, like Lnp, it is likely that ATL3 is pulled along in the experiments where Lnp is redistributed, and it could therefore also explain the observed phenotypes. RNF26 has already been identified as a linker between VIM and the perinuclear ER (Cremer et al., 2022), but we think it is inevitable that there is also a linkage of the tubular ER with VIM, because VIM is retracted from the cell periphery when the tubular ER network is lost and converted into a sheet-like structure. Altogether, from this study the tubular ER seems to provide anchoring points where VIM can make connections with the ER network. 3WJs are possible anchoring points of the tubular ER network to VIM, with Lnp and ATL3 as interesting linker candidates. However, it could also be that the changes in the VIM network we observed when we relocalised Lnp or depleted ATL are indirect results

that are caused by the changes in the ER morphology and not necessarily directly by these ER shaping proteins.

Besides this direct connection between the ER and VIM, lysosomes could act as an indirect linkage between the two. We confirmed that VIM clusters lysosomes perinuclearly and restricts their peripheral localisation. This could in turn affect the ER morphology, because lysosomes regulate the structure and distribution of the ER (Lu et al., 2022). We have not looked further into a possible indirect effect of VIM on the ER through lysosomes, but it would definitely be an interesting study. Live cell imaging could be used to investigate if the lysosome assisted ER dynamics is different in VIM depleted cells.

MATERIALS & METHODS

Table 1 Key resources

Reagent type (species) or resource	Designation	Source or reference	Identifiers
Antibody	Anti-Vimentin-V9 (mouse	Sigma-Aldrich	
Antibody	Anti-α-tubulin YL1/2 (Rat monoclonal)	Pierce	Pierce: MA1-80017; RRID:AB_2210201
Antibody	Anti-Calnexin (Rabbit polyclonal)	Abcam	Abcam Cat# ab22595, RRID:AB_2069006
Antibody	Anti-Lamtor4 (Rabbit monoclonal)	Cell Signaling (CST)/ Bioke	Cell Signaling Technology Cat# 12284, RRID:AB_2797870
Antibody	Anti-GFP (Mouse monoclonal)	Sigma-Aldrich	Sigma-Aldrich Cat# 11814460001
Antibody	Anti-GFP (rabbit polyclonal)	Abcam	Abcam Cat# ab290
Antibody	Anti-HA (rat		
Antibody	Alexa Fluor 405-, 488-, 594- and 647-secondaries	Molecular Probes/ Thermo Fisher Scientific	Molecular Probes Cat# A-11007, RRID:AB_141374; Cat# A-11034, RRID:AB_2576217; Cat# A-32723, RRID:AB_2633275; Cat# A-31553, RRID:AB_221604; Cat# A-11029, RRID:AB_138404; Cat# A-11032, RRID:AB_2534091; Cat# A-11006, RRID:AB_141373; Thermo Fisher Scientific Cat# A-11012, RRID:AB_2534079
Sequence-based reagent	siRNA against Luciferase		5’-CGUACGCGGAAUACUUCGA-3’
Sequence-based reagent	siRNA against VAP A	Venditti et al., 2019	5’-CCACAGACCUCAAAUUCAA-3’
Sequence-based reagent	siRNA against VAP B	Venditti et al., 2019	5’-GUAAGAGGCUGCAAGGUGA-3’
Sequence-based reagent	siRNA #1 against ATL2	Rismanchi et al., 2008	5’-GGAGCUAUCCUUAUGAACAUUCAUA-3’
Sequence-based reagent	siRNA #2 against ATL2	Rismanchi et al., 2008	5’-UCCUGGUCUUAAAGUUGCAACUAAU-3’
Sequence-based reagent	siRNA #1 against ATL3	Rismanchi et al., 2008	5’-GCCCUGACUUUGAUGGGAAAUUAAA-3’
Sequence-based reagent	siRNA #2 against ATL3	Rismanchi et al., 2008	5’-GGGCUACAUCAGGUAUUCUGGUCAA-3’
Chemical compound	Nocodazole	Sigma-Aldrich	Sigma-Aldrich Cat # M1404-10MG
Chemical compound	Rapalog (A/C Heterodimerizer)	Takara	Takara, Cat # 635,056

Reagent type (species) or resource	Designation	Source or reference	Identifiers
Recombinant DNA reagent	VIM-mNeonGreen	This work	
Recombinant DNA reagent	2xFKBP-mCherry-VIM	This work	
Recombinant DNA reagent	GFP-FKBP-Sec61β	This work	
Recombinant DNA reagent	RTN4-GFP-FKBP	This work	
Recombinant DNA reagent	LNP-eGFP-2xFKBP	This work	
Recombinant DNA reagent	HA-KIF5A-FRB	This work	
Recombinant DNA reagent	FRB-TagBFP-GCN4-ppKin14Ulb (plasmid)	This work	
Recombinant DNA reagent	pB80-FRB-HA-GCN4-ppKin14 (plasmid)	This work	

Cell Culture

The cells (COS7/HeLa/MCF7) were cultured in 6-well plates and grown in media, consisting of 90% Dulbecco's modified Eagle's medium (DMEM), 10% foetal bovine serum (FBS, GE Healthcare) and 1% penicillin and streptomycin (Sigma-Aldrich), and incubated at 37 °C in 5% CO_2 atmosphere. For immunofluorescence (IF) experiments, the cells were plated in a 24-well plate containing a 10 mm cover glass.

Cloning LNP-eGFP-2xFKBP construct

To create a construct that would enable us to manipulate the localisation of LNP, both LNP-eGFP SII and VHH-eGFP-2xFKBP constructs were digested with XhoI and BsrGI. The gel-purified bands corresponding with LNP-eGFP and the linear vector containing 2xFKBP were annealed with T4 ligation to generate the final LNP-eGFP-2xFKBP construct.

DNA & siRNA transfection

FuGENE 6 (Promega) was used for transfection of the cells with the plasmids and RNAiMAX (Thermo Fisher Scientific) was used to transfect the cells with siRNAs. The recommended reagent/DNA, reagent /siRNA ratios were used according to the manufacturer's instructions. The cells were transfected with 0.5 µg per construct per well (24-well plate) 24 hrs before fixation. For siRNA depletion of VIM, ATL2/3 and VAP A/B, the cells were transfected with 20 µM of the siRNAs 72 hrs before fixation.

Drug Treatments

To induce dimerization of constructs containing FRB or FKBP domains, cells were treated with Rapalog. In the experiments where VIM was pulled, cells were treated with 100 nM Rapalog for 1.5 hours. For the experiments where Sec61β or Lnp was pulled, cells were treated with 200 nM Rapalog for 2 hours. To depolymerise MTs, cells were treated with 10 µM Nocodazole on ice for either 2 or 4 minutes and immediately fixed after treatment.

Immunofluorescence staining

The cells were fixed at room temperature (RT) for 10 min with pre-warmed (37 °C) PBS containing 4% paraformaldehyde (PFA), 0.1% glutaraldehyde and 4% sucrose (cells stained for lysosomes were fixed with 4% PFA). After washing twice with 1X PBS, the cells were permeabilised with 0.5% Triton X-100 in PBS for 5 min. It was washed again twice with PBS and thereafter the samples were quenched with 100 mM $NaBH_4$ in PBS three times 5 min. After washing another two times with PBS, the coverslips

were incubated in blocking solution (2% bovine serum albumin (BSA) and 0.05% Tween-20 in 1X PBS) for 45-60 min at RT on a shaker. After blocking, the coverslips were transferred to a stand covered in parafilm (cell-side up) and incubated for 1 hr at RT with primary antibodies (1:200 dilution in blocking solution). The coverslips were washed four times 2 min with washing solution (0.05% Tween-20 in 1X PBS) and subsequently incubated for 1 hr at RT with secondary antibodies. After washing another four times 2 min with washing solution, the coverslips were transferred to a tissue to dry. Small drops of Prolong mounting medium were applied on a glass slide and the coverslips were mounted on it (cell-side down).

Image acquisition

Fixed cells of the experiments handling the effect of VIM on the ER and lysosomes were imaged with a Nikon Eclipse Ni upright fluorescence microscope equipped with a DS-Qi2 CMOS camera (Nikon), an Intensilight C-HGFI epi-fluorescence illuminator (Nikon), Plan Apo Lambda 100×NA 1.45 oil objectives (Nikon) and driven by NIS-Elements Br software (Nikon).

Images of fixed cells of the experiments handling the effect of the ER on VIM and MTs were acquired with either a Zeiss LSM700 confocal microscope, equipped with a mercury lamp, a 63x oil objective and driven by ZEN software, or with Leica TCS SP8 STED 3 X microscope driven by LAS X software using HC PL APO 100 x/1.4 oil STED WHITE objective, white light laser (633 nm) for excitation and 775 nm pulsed lased for depletion.

Quantifications

The microtubule and VIM densities were quantified by measuring the intensity signal of the whole cell and subtracting the background signal. All values were normalised by dividing it with the average value of the control condition. The cell area and circularity were determined by outlining the cell and calculating the values for these drawn cell outlines. The VIM spreading was calculated by dividing the area of the VIM signal by the total area of the cell. All these things were quantified using Fiji/ImageJ.

Lysosome Distribution

To analyse the lysosome distribution the Fiji plugin MTrackJ (Meijering et al., 2012) was used. The outline of the cells was determined manually. For every detected lysosome, the radial distance to the cell centre and periphery were determined. The distance to the centre was divided by the total distance to get the relative distance to the centre for every lysosome. These values were binned into 20 groups and that resulted in the distribution plots in Figure 2.

REFERENCES

Chen, S., Desai, T., McNew, J. A., Gerard, P., Novick, P. J., & Ferro-Novick, S. (2015). Lunapark stabilizes nascent three-way junctions in the endoplasmic reticulum. *Proceedings of the National Academy of Sciences*, *112*(2), 418–423. https://doi.org/10.1073/pnas.1423026112

Cremer, T., Voortman, L. M., Bos, E., van Elsland, D. M., ter Haar, L. R., Koning, R. I., Berlin, I., & Neefjes, J. (2022). Vimentin intermediate filaments organize organellar architecture in response to ER stress. *BioRxiv*, 2022.03.24.485587. https://doi.org/10.1101/2022.03.24.485587

Goyal, U., & Blackstone, C. (2013). Untangling the web: Mechanisms underlying ER network formation. *Biochimica et Biophysica Acta (BBA) - Molecular Cell Research*, *1833*(11), 2492–2498. https://doi.org/https://doi.org/10.1016/j.bbamcr.2013.04.009

Guo, Y., Li, D., Zhang, S., Yang, Y., Liu, J.-J., Wang, X., Liu, C., Milkie, D. E., Moore, R. P., Tulu, U. S., Kiehart, D. P., Hu, J., Lippincott-Schwartz, J., Betzig, E., & Li, D. (2018). Visualizing Intracellular Organelle and Cytoskeletal Interactions at Nanoscale Resolution on Millisecond Timescales. *Cell*, *175*(5), 1430-1442.e17. https://doi.org/10.1016/j.cell.2018.09.057

Helle, S. C. J., Kanfer, G., Kolar, K., Lang, A., Michel, A. H., & Kornmann, B. (2013). Organization and function of membrane contact sites. *Biochimica et Biophysica Acta (BBA) - Molecular Cell Research*, *1833*(11), 2526–2541. https://doi.org/https://doi.org/10.1016/j.bbamcr.2013.01.028

Hu, X., Wu, F., Sun, S., Yu, W., & Hu, J. (2015). Human atlastin GTPases mediate differentiated fusion

of endoplasmic reticulum membranes. *Protein & Cell*, *6*(4), 307–311. https://doi.org/10.1007/s13238-015-0139-3

James, C., & Kehlenbach, R. H. (2021). The Interactome of the VAP Family of Proteins: An Overview. In *Cells* (Vol. 10, Issue 7). https://doi.org/10.3390/cells10071780

Janmey, P. A., Euteneuer, U., Traub, P., & Schliwa, M. (1991). Viscoelastic properties of vimentin compared with other filamentous biopolymer networks. *Journal of Cell Biology*, *113*(1), 155–160. https://doi.org/10.1083/jcb.113.1.155

Ketema, M., Kreft, M., Secades, P., Janssen, H., & Sonnenberg, A. (2013). Nesprin-3 connects plectin and vimentin to the nuclear envelope of Sertoli cells but is not required for Sertoli cell function in spermatogenesis. *Molecular Biology of the Cell*, *24*(15), 2454–2466. https://doi.org/10.1091/mbc.e13-02-0100

Lu, M., van Tartwijk, F. W., Lin, J. Q., Nijenhuis, W., Parutto, P., Fantham, M., Christensen, C. N., Avezov, E., Holt, C. E., Tunnacliffe, A., Holcman, D., Kapitein, L., Schierle, G. S. K., & Kaminski, C. F. (2022). The structure and global distribution of the endoplasmic reticulum network are actively regulated by lysosomes. *Science Advances*, *6*(51), eabc7209. https://doi.org/10.1126/sciadv.abc7209

Lynch, C. D., Lazar, A. M., Iskratsch, T., Zhang, X., & Sheetz, M. P. (2012). Endoplasmic spreading requires coalescence of vimentin intermediate filaments at force-bearing adhesions. *Molecular Biology of the Cell*, *24*(1), 21–30. https://doi.org/10.1091/mbc.e12-05-0377

Meijering, E., Dzyubachyk, O., & Smal, I. (2012). Chapter nine - Methods for Cell and Particle Tracking. In P. M. B. T.-M. in E. conn (Ed.), *Imaging and Spectroscopic Analysis of Living Cells* (Vol. 504, pp. 183–200). Academic Press. https://doi.org/https://doi.org/10.1016/B978-0-12-391857-4.00009-4

Patteson, A. E., Vahabikashi, A., Pogoda, K., Adam, S. A., Mandal, K., Kittisopikul, M., Sivagurunathan, S., Goldman, A., Goldman, R. D., & Janmey, P. A. (2019). Vimentin protects cells against nuclear rupture and DNA damage during migration. *Journal of Cell Biology*, *218*(12), 4079–4092. https://doi.org/10.1083/jcb.201902046

Rismanchi, N., Soderblom, C., Stadler, J., Zhu, P.-P., & Blackstone, C. (2008). Atlastin GTPases are required for Golgi apparatus and ER morphogenesis. *Human Molecular Genetics*, *17*(11), 1591–1604. https://doi.org/10.1093/hmg/ddn046

Robert, A., Tian, P., Adam, S. A., Kittisopikul, M., Jaqaman, K., Goldman, R. D., & Gelfand, V. I. (2019). Kinesin-dependent transport of keratin filaments: a unified mechanism for intermediate filament transport. *The FASEB Journal*, *33*(1), 388–399. https://doi.org/https://doi.org/10.1096/fj.201800604R

Schwarz, D. S., & Blower, M. D. (2016). The endoplasmic reticulum: structure, function and response to cellular signaling. *Cellular and Molecular Life Sciences*, *73*(1), 79–94. https://doi.org/10.1007/s00018-015-2052-6

Tikhomirova, M. S., Kadosh, A., Saukko-Paavola, A. J., Shemesh, T., & Klemm, R. W. (2022). A role for endoplasmic reticulum dynamics in the cellular distribution of microtubules. *Proceedings of the National Academy of Sciences*, *119*(15), e2104309119. https://doi.org/10.1073/pnas.2104309119

Venditti, R., Rega, L. R., Masone, M. C., Santoro, M., Polishchuk, E., Sarnataro, D., Paladino, S., D'Auria, S., Varriale, A., Olkkonen, V. M., Di Tullio, G., Polishchuk, R., & De Matteis, M. A. (2019). Molecular determinants of ER–Golgi contacts identified through a new FRET–FLIM system. *Journal of Cell Biology*, *218*(3), 1055–1065. https://doi.org/10.1083/jcb.201812020

Wang, N., Clark, L. D., Gao, Y., Kozlov, M. M., Shemesh, T., & Rapoport, T. A. (2021). Mechanism of membrane-curvature generation by ER-tubule shaping proteins. *Nature Communications*, *12*(1), 568. https://doi.org/10.1038/s41467-020-20625-y

Wang, S., Tukachinsky, H., Romano, F. B., & Rapoport, T. A. (2016). Cooperation of the ER-shaping proteins atlastin, lunapark, and reticulons to generate a tubular membrane network. *ELife*, *5*, e18605. https://doi.org/10.7554/eLife.18605

Waterman-Storer, C. M., & Salmon, E. D. (1998). Endoplasmic reticulum membrane tubules are

distributed by microtubules in living cells using three distinct mechanisms. *Current Biology*, *8*(14), 798–807. https://doi.org/https://doi.org/10.1016/S0960-9822(98)70321-5

Wu, H., Carvalho, P., & Voeltz, G. K. (2018). Here, there, and everywhere: The importance of ER membrane contact sites. *Science (New York, N.Y.)*, *361*(6401), eaan5835. https://doi.org/10.1126/science.aan5835

Zhang, H., & Hu, J. (2016). Shaping the Endoplasmic Reticulum into a Social Network. *Trends in Cell Biology*, *26*(12), 934–943. https://doi.org/10.1016/j.tcb.2016.06.002

Zhou, X., He, Y., Huang, X., Guo, Y., Li, D., & Hu, J. (2019). Reciprocal regulation between lunapark and atlastin facilitates ER three-way junction formation. *Protein & Cell*, *10*(7), 510–525. https://doi.org/10.1007/s13238-018-0595-7

SUPPLEMENTARY FIGURES

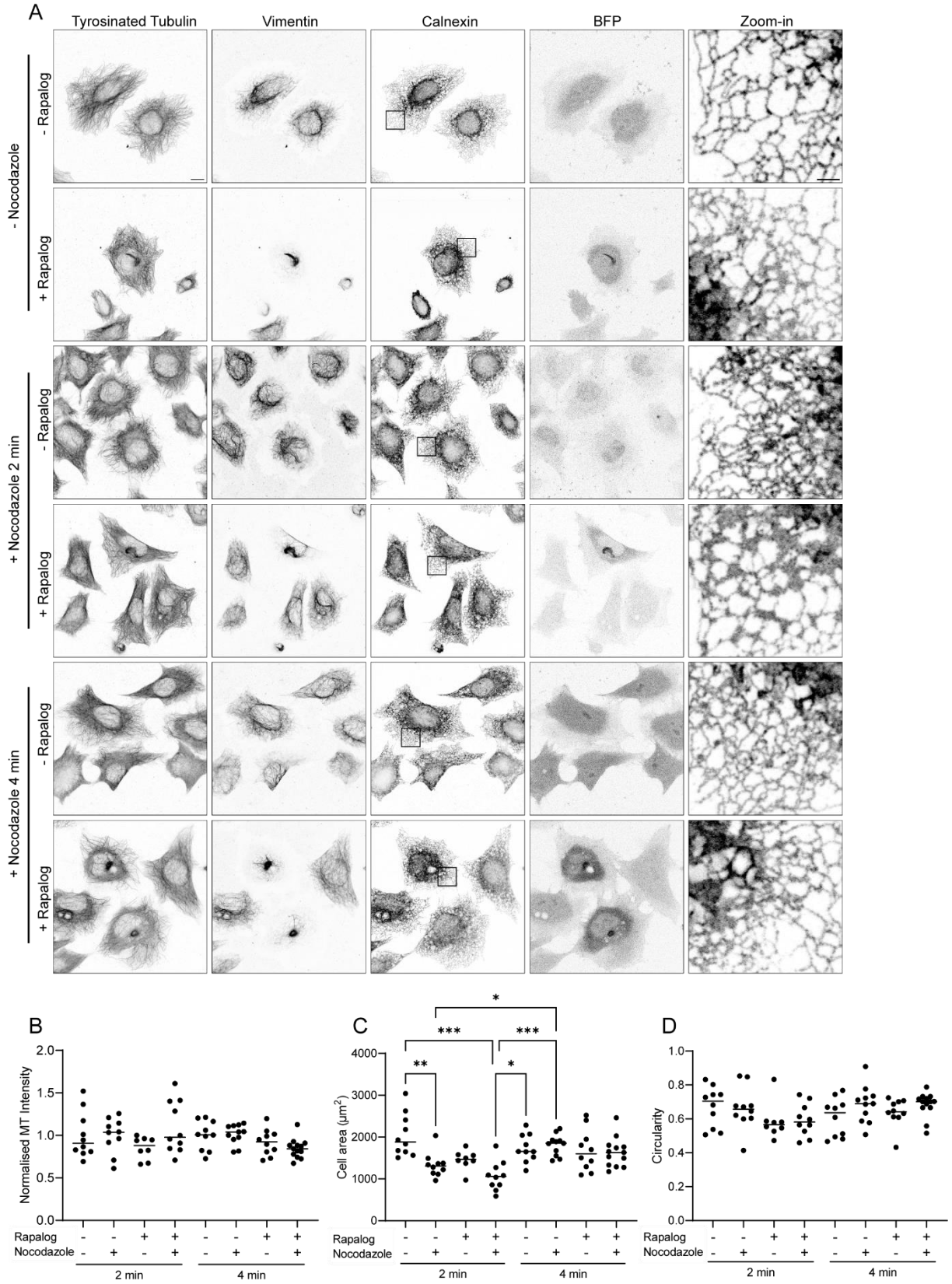

Figure S1 The number and size of ER sheets increases when Vimentin is repositioned to the cell centre and microtubules are depolymerised shortly. (A) Immunofluorescence images of HeLa cells transfected with 2xFKBP-mCherry-Vimentin and FRB-TagBFP-GCN4-ppKin14Ulb and stained for tyrosinated tubulin, Vimentin and Calnexin. The cells were treated with rapalog (1.5 hrs) and nocodazole on ice, indicated on the side. The boxes indicate the areas shown in the zoom-ins. Scale bar 10 µm, scale bar zoom-in 2 µm. (B) Quantification of the microtubule intensities, normalised to the cells treated with neither of the compounds. (C) Quantification of the cell area. (D) Quantification of the cell circularity. In the graphs, only significant differences are indicated. * P<0.05, ** P<0.01, *** P<0.001.

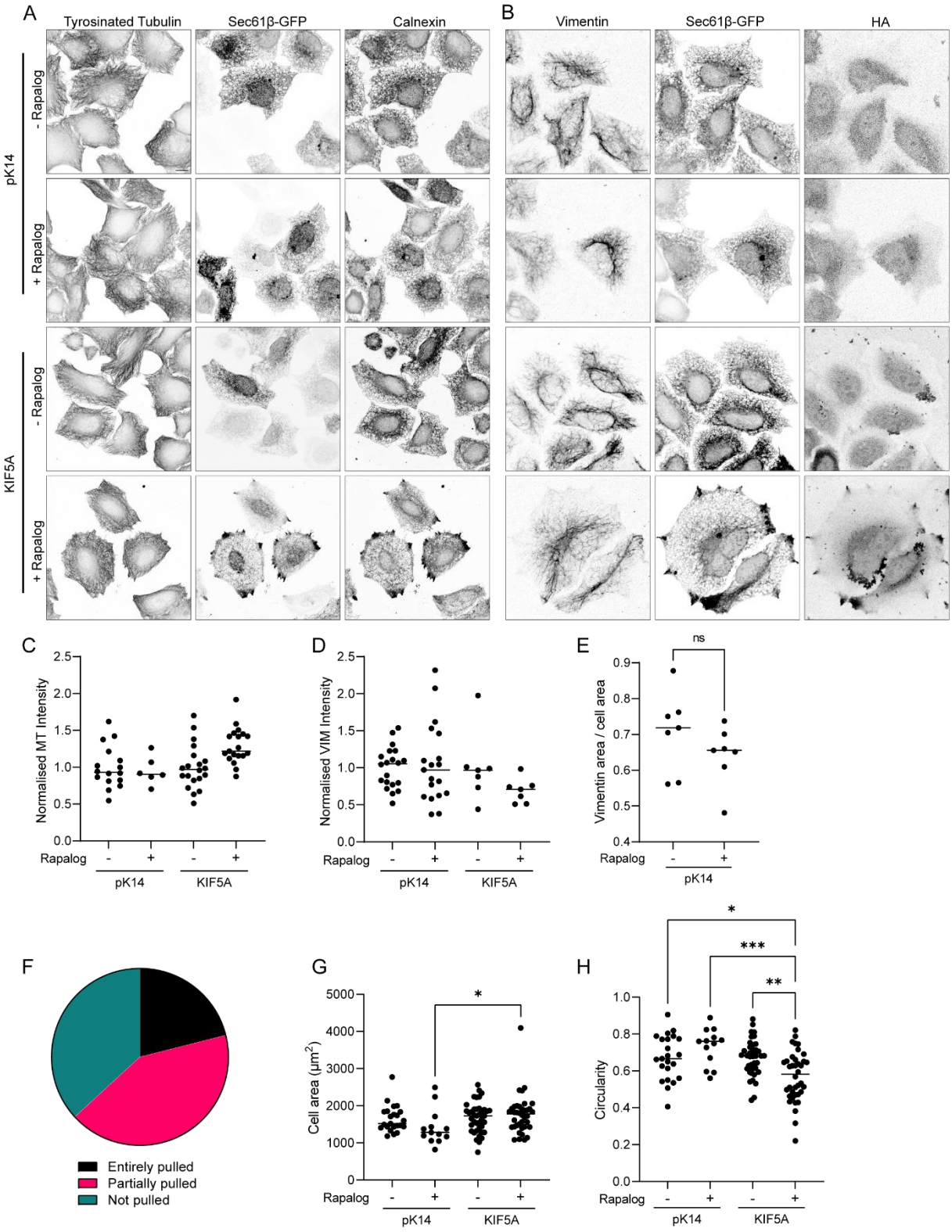

Figure S2 Repositioning the general ER membrane protein Sec61β to the cell periphery affects the Vimentin network. (A) Immunofluorescence images of HeLa cells transfected with GFP-FKBP-Sec61β and either FRB-HA-GCN4-ppKin14 or HA-KIF5A-FRB and stained for tyrosinated tubulin, GFP and Calnexin. The cells were treated with rapalog for 2 hours to induce translocation. Scale bar 10 µm. (B) Same as in (A), but here stained for Vimentin, GFP and HA. (C) Quantification of the microtubule intensities normalised to the cells not treated with Rapalog. (D) Quantification of the Vimentin intensities normalised to the cells not treated with Rapalog. (E) Quantification of the Vimentin spreading in the cells transfected with the rapalog inducible pK14 motor. (F) Distribution of the different observed phenotypes regarding the Vimentin network being pulled along with Sec61β (n=19). (G) Quantification of the cell area. (H) Quantification of the cell circularity. * P<0.05, ** P<0.01, *** P<0.001.

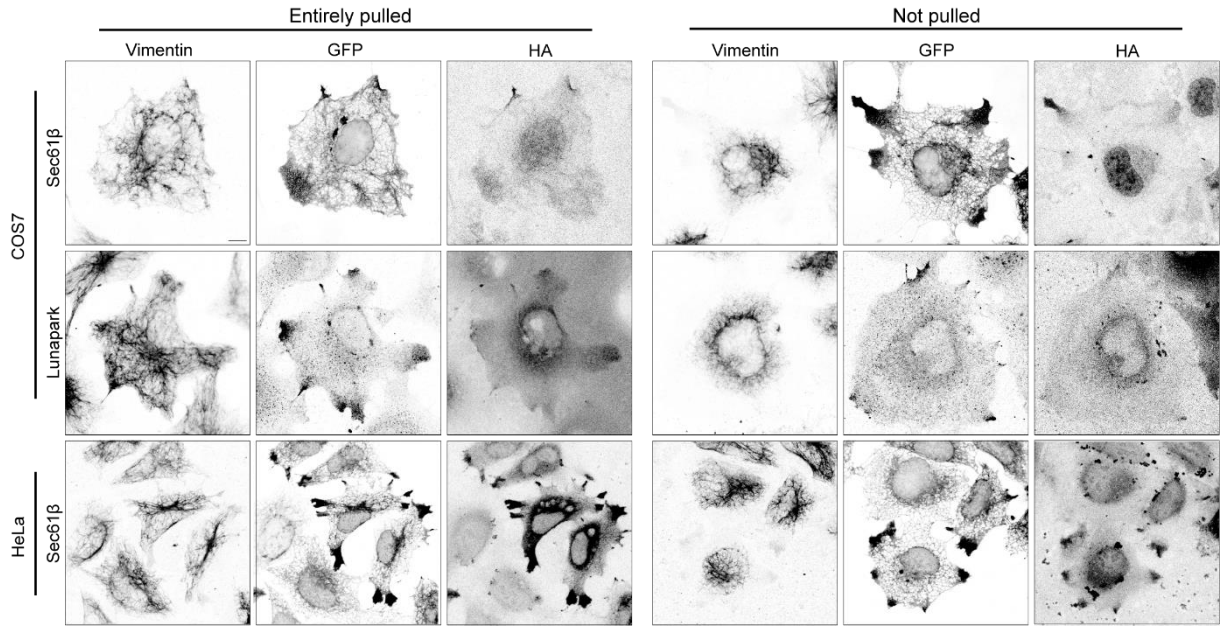

Figure S3 Examples of the different phenotypes observed when the different ER proteins are repositioned to the cell periphery. Immunofluorescence images of COS7 and HeLa cells transfected with either GFP-FKBP-Sec61β or LNP-GFP-2xFKBP and HA-KIF5A-FRB and stained for Vimentin, GFP and HA. All of the shown cells were treated with rapalog for 2 hours to induce translocation. Scale bar 10 μm.

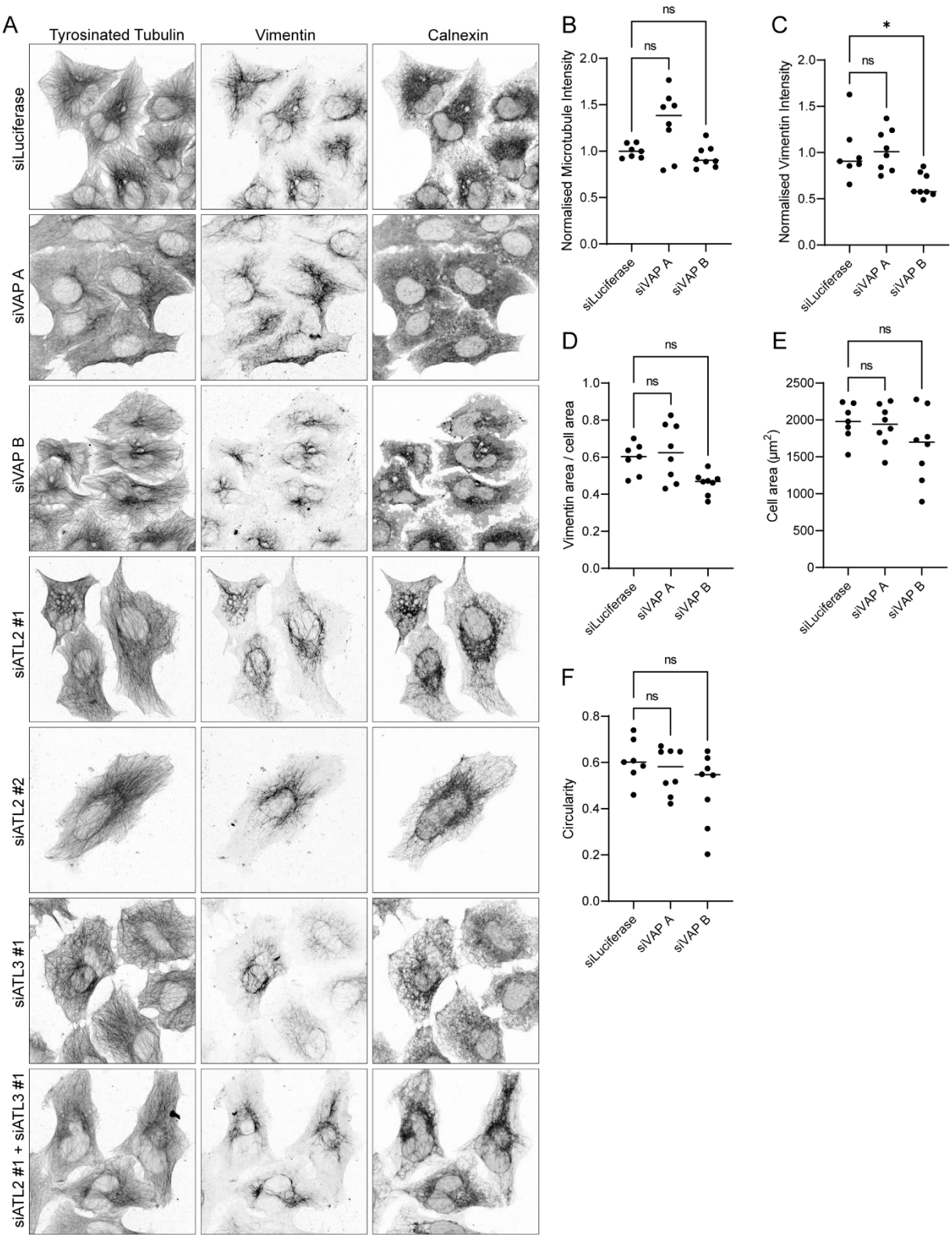

Figure S4 Knock-down of members of the ER shaping protein families VAPs and Atlastins affects the Vimentin and microtubule networks. (A) Immunofluorescence images of HeLa cells treated with the indicated siRNAs and stained for tyrosinated tubulin, Vimentin and Calnexin. Scale bar 10 µm. (B) Quantification of the microtubule intensities, normalised to the cells treated with siLuciferase. (C) Quantification of the Vimentin intensities normalised to the cells treated with siLuciferase. (D) Quantification of the Vimentin spreading. (E) Quantification of the cell area. (F) Quantification of the cell circularity. * P<0.05.